Magnetic-Field Switching of Crystal Structure in an Orbital-Spin-Coupled System: MnV_2O_4

K. Adachi,[1] T. Suzuki,[1] K. Kato,[2,3] K. Osaka,[2] M. Takata,[2,3] and T. Katsufuji[1,4]

[1]*Department of Physics, Waseda University, Tokyo 169-8555, Japan*
[2]*JASRI/SPring-8, Hyogo 679-5198, Japan*
[3]*CREST, Japan Science and Technology Corporation, Saitama 332-0012, Japan*
[4]*PRESTO, Japan Science and Technology Corporation, Saitama 332-0012, Japan*

(Received 26 April 2005; published 2 November 2005)

We studied the magnetic and structural properties of spinel MnV_2O_4, which has $S = 5/2$ spin with no orbital degrees of freedom on the Mn^{2+} site and $S = 1$ spin and three orbital degrees of freedom on the V^{3+} site. We found that the ferrimagnetic ordering at $T_N = 56.5$ K and the structural phase transition at $T_s = 53.5$ K are closely correlated in this compound and found a switching of crystal structure between cubic and tetragonal phases by the magnetic field. This phenomenon can be explained by the coupling between orbital and spin degrees of freedom in the t_{2g} states of the V site.

DOI: 10.1103/PhysRevLett.95.197202 PACS numbers: 75.80.+q, 61.10.−i, 75.50.Gg

There has been an emerging interest in the coupling between orbital and spin degrees of freedom in strongly correlated electron systems. Orbital degrees of freedom arise when degenerate states ($3d$ orbitals, for example) with the number of degeneracy n are occupied by a number of electrons other than n or $2n$. These orbital degrees of freedom often dominate the crystal structure. For example, the ordering of orbitals leads to lattice distortion in a lower symmetry. The orbital degrees of freedom and the resultant lattice distortion give rise to more interesting physics when they are coupled with spin degrees of freedom. This coupling arises not only from conventional spin-orbit coupling but also from the fact that the occupation of specific orbitals with geometrical anisotropy prefers specific types of magnetic interaction in specific directions (the so-called Kugel-Khomskii-type coupling) [1]. A typical example of the latter coupling is found in perovskite manganites [2], in which doubly degenerate e_g orbitals of the Mn $3d$ state are occupied by one electron. For example, $LaMnO_3$ shows the so-called A-type (layered-type) antiferromagnetic ordering, which is dominated by the staggered-type ordering of Mn $3d_{x^2}$ ($3d_{y^2}$) orbitals. In hole-doped perovskite manganites, on the other hand, when the magnetic field aligns the Mn spins in the same direction, the Mn orbital state changes, resulting in the change of its crystal structure as well as in the substantial decrease of electrical resistivity, often called ''colossal magnetoresistance.'' Magnetoelectric phenomena recently discovered in several manganites [3,4] can be also attributed to the coupling between e_g orbitals and spins.

Such orbital-spin coupling occurs not only in the doubly degenerate e_g orbital but also in the triply degenerate t_{2g} orbital of the d state. Indeed, several results related to the orbital-spin coupling have been reported in perovskite [5] and spinel [6] vanadates having two electrons in the t_{2g} orbital. However, there is almost no report on the control of the orbital state by the magnetic field in these t_{2g} systems. The main problem is that most of the t_{2g} systems are heavily antiferromagnetic and, thus, are not sensitive to the magnetic field.

Here we overcome this obstacle by putting additional magnetic ions in the crystal and enhancing the effect of the magnetic field. The compound studied here is spinel MnV_2O_4. In this compound, the A site of the spinel structure (AB_2C_4) is occupied by the Mn^{2+} ion, which is in the $3d^5$ high-spin configuration with no orbital degrees of freedom, and can be regarded as a simple $S = 5/2$ spin. On the other hand, the B site is occupied by the V^{3+} ion, which takes the $3d^2$ high-spin configuration in the triply degenerate t_{2g} orbital, and has orbital degrees of freedom. According to previous studies [7,8], MnV_2O_4 exhibits a ferrimagnetic ordering at $T_N = 56$ K, where the magnetic moments of the Mn and the V sites align to the opposite direction, and then a structural phase transition from a cubic to a tetragonal phase at $T_s = 53$ K. Associated with this structural phase transition, the spin structure changes from a collinear Néel configuration to a noncollinear ''triangular'' structure. These results imply that the structural phase transition at 53 K is dominated by the orbital degrees of freedom on the V site, and there is an interplay between orbital and spin degrees of freedom in this compound.

Polycrystalline samples of MnV_2O_4 and doped $Mn_{1-x}Zn_xV_2O_4$ and $Mn(V_{1-x}Al_x)_2O_4$ were synthesized by a conventional solid-state-reaction method in a sealed quartz tube at 1100 °C. X-ray powder diffraction measurement using a synchrotron radiation x-ray source was carried out at SPring-8 BL02B2 with the wavelength 0.7500 Å [9]. Magnetic susceptibility was measured by a SQUID magnetometer. Lattice striction measurement was done by a strain-gauge technique under magnetic field.

First, we show the synchrotron x-ray powder diffraction patterns of MnV_2O_4 and the Rietveld analysis above and below the structural-phase-transition temperature T_s in Fig. 1. The space group used for the analysis above T_s is $Fd\bar{3}m$, a simple cubic spinel structure, and $I4_1/amd$ below T_s, which is the same as that of ZnV_2O_4 at low tempera-

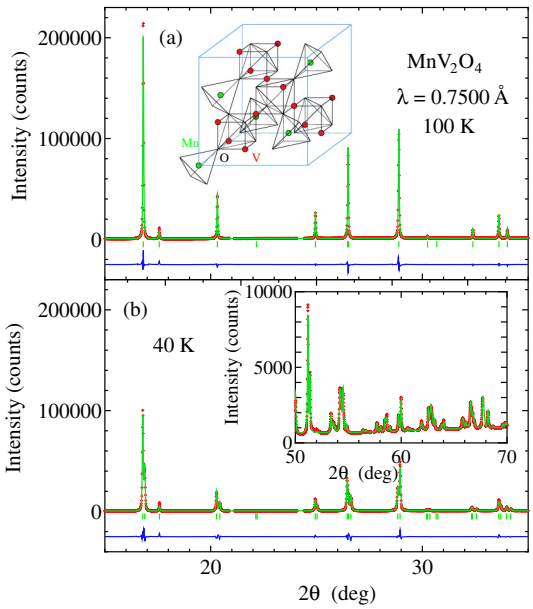

FIG. 1 (color online). Synchrotron x-ray powder diffraction patterns (plus marks) and Rietveld refinement patterns (solid lines) of MnV_2O_4 at (a) 100 K ($Fd\bar{3}m$) and (b) 40 K ($I4_1/amd$). The vertical marks indicate the position of Bragg peaks, and the solid line at the bottom corresponds to the difference between observed and calculated intensities. The inset in the lower panel is the expanded figure at higher angles $2\theta = 50$–$70°$.

tures [10]. The fitting result is almost satisfactory as shown in Fig. 1, and the atomic parameters from the fitting are summarized in Table I. The V-O bond length in the low-temperature phase obtained from the fitting is 1.990(2) Å along the c axis and 2.034(1) Å within the ab plane, indicating that the VO_6 octahedral is compressed along the c direction by 2% below T_s. This distortion splits the triply degenerate t_{2g} orbitals into an xy orbital with a lower energy and doubly degenerate yz and zx orbitals with a higher energy. Thus, the degeneracy of the V site with two electrons is not lifted only with this distortion but another mechanism is required for a stable electronic state. We also

TABLE I. Atomic parameters of MnV_2O_4 at 100 K [$Fd\bar{3}m$, $a = 8.508\,36(8)$ Å] and 40 K [$I4_1/amd$, $a = 6.025\,01(5)$ Å, $c = 8.459\,17(8)$ Å] from synchrotron x-ray powder diffraction refinements. $R_{wp} = 8.14$ and $R_e = 2.41$ for the 100 K data, and $R_{wp} = 8.93$ and $R_e = 2.68$ for the 40 K data.

Atom	Site	x	y	z	B(Å^2)
	MnV_2O_4	100 K	$Fd\bar{3}m$		
Mn	8a	0	0	0	0.20(1)
V	16d	0.625	0.625	0.625	0.11(1)
O	32e	0.3883(1)	0.3883(1)	0.3883(1)	0.38(3)
	MnV_2O_4	40 K	$I4_1/amd$		
Mn	4a	0	0.75	0.125	0.14(1)
V	8d	0	0	0.5	0.07(1)
O	16h	0	0.0243(3)	0.2655(2)	0.26(3)

tried the fitting by $I4_1/a$, in which the orbital ordering proposed by Tsunetsugu *et al.* [11] for ZnV_2O_4 is taken into account so that reflections m in the (110) plane and diamond glides d do not exist. We could find no additional peak that should exist only in $I4_1/a$. Note that the difference between $I4_1/amd$ and $I4_1/a$ phases is only one additional freedom on the oxygen position, and, thereby, we could possibly miss the additional peaks in the x-ray powder diffraction data [12]. For now, the existence of such orbital ordering as proposed by Tsunetsugu *et al.* in MnV_2O_4 is still an open question.

Figure 2 shows the temperature (T) dependence of lattice striction ($\Delta L/L$) and magnetization (M) in MnV_2O_4. With decreasing T (in the cooling run), M sharply increases at 56.5 K, corresponding to the ferrimagnetic ordering. However, $M(T)$ has a maximum around 55 K and decreases with further decreasing temperature. At 53.5 K, there is a sharp dip of $M(T)$, which corresponds to the structural phase transition (T_s) [7]. On the other hand, $\Delta L/L$ starts decreasing below $T_N = 56.5$ K and then shows another anomaly at $T_s = 53.5$ K. It is no surprise to see an anomaly of $\Delta L/L$, which corresponds to the variation of the average lattice constant, at the structural phase transition $T_s = 53.5$ K. However, the onset of the decrease of $\Delta L/L$ at $T_N = 56.5$ K is an unexpected result. This means that the lattice first begins to contract below T_N with keeping its cubic symmetry, and then it is distorted

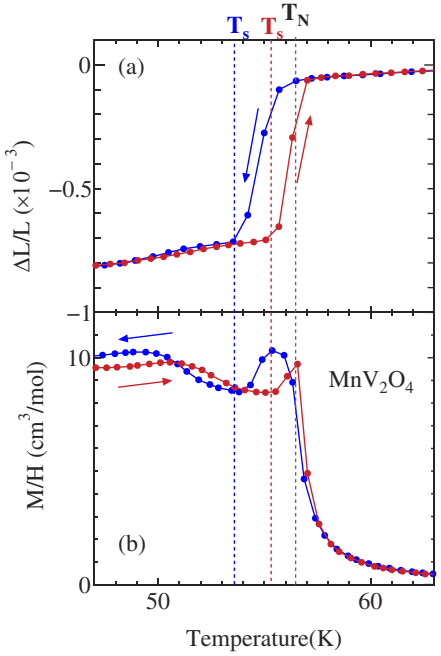

FIG. 2 (color online). Temperature dependence of (a) lattice striction ($\Delta L/L$) and (b) magnetization (M) under 100 G. M is given per MnV_2O_4 mole. Two lines at each panel are the data taken in the cooling run and the warming run. The dotted lines refer to the ferromagnetic-ordering temperature T_N and the structural-phase-transition temperature T_s, which is defined for both cooling and warming runs.

into a tetragonal symmetry below T_s. These results indicate a close correlation between T_N and T_s in MnV_2O_4. There is a thermal hysteresis in both $\Delta L/L$ and M, and, in the warming run, the anomalies of $\Delta L/L$ and $M(T)$ corresponding to T_s are observed at 55.5 K.

The close correlation between T_N and T_s in this compound motivated us to measure the lattice striction $\Delta L/L$ under magnetic field H. As shown in Fig. 3(a), the T dependence of $\Delta L/L$ shows almost a parallel shift to higher T with increasing H. This means that the structural-phase-transition temperature T_s, as shown by the arrows, shifts to higher T with magnetic field. Figure 3(b) shows the H dependence of $\Delta L/L$ with a constant T. A large change of $\Delta L/L$ under magnetic field is observed, which indicates a magnetic-field switching of crystal structure from a cubic to a tetragonal phase. This structural switching with magnetic field has a hysteresis, similarly to the thermal hysteresis of the structural change. The results are summarized in Fig. 3(c) as a phase diagram in the space of magnetic field and temperature with a large hysteresis region.

Note that this structural phase transition with magnetic field in MnV_2O_4 is different from a conventional magnetostriction by magnetic anisotropy, which is observed in many magnets. First, the crystal lattice begins to contract below T_N with keeping its cubic symmetry in MnV_2O_4, and this is hard to explain by magnetic anisotropy. Second, the structural phase transition is of the first order, as shown by its thermal and magnetic-field hysteresis, and this is also

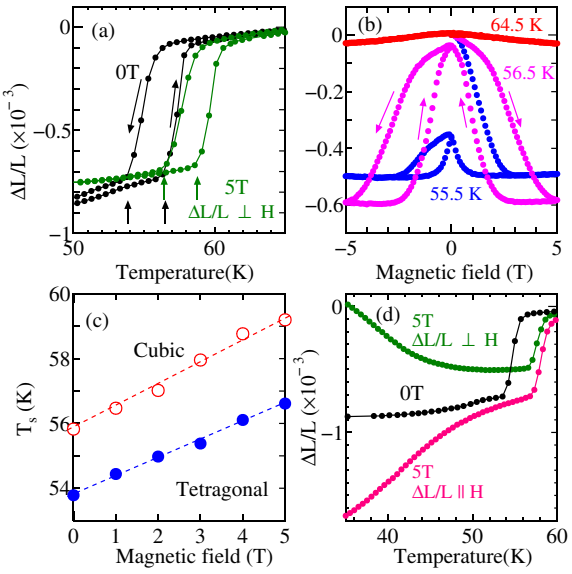

FIG. 3 (color online). (a) Temperature dependence of lattice striction $\Delta L/L$ at 0 and 5 T around T_s. The arrows show T_s in the cooling and warming runs at each magnetic field. (b) Magnetic-field dependence of lattice striction $\Delta L/L$ at three different temperatures. (c) Phase diagram of crystal structure as a function of temperature and magnetic field. (d) Temperature dependence of striction $\Delta L/L$ below T_s at 0 T, at 5 T with $\Delta L/L \perp H$, and at 5 T with $\Delta L/L \parallel H$. The measurement was done in cooling runs.

hard to reconcile with the magnetostriction by magnetic anisotropy. Third, the cooperative nature of this phase transition is clearly seen in the comparison between undoped MnV_2O_4 and doped MnV_2O_4, as discussed later.

Such a magnetic-field switching of crystal structure between different symmetries is rare, except for those occurring in perovskite mangatnies [13,14]. However, there is a critical difference between the phase transition in perovskite manganite and present MnV_2O_4. In perovskite manganites, a crystal symmetry changes into a higher one with magnetic field, for example, from orthorhombic to trigonal [13] or from a charge-ordered phase with superlattice modulation to a charge-disordered phase [14]. On the other hand, the crystal symmetry is lowered from cubic to tetragonal under magnetic field in MnV_2O_4.

It is informative to compare the present compound MnV_2O_4 with isostructural ZnV_2O_4, which has a nonmagnetic Zn ion on the A site of the spinel structure [6,10,15]. In ZnV_2O_4, there is a strong antiferromagnetic V-V interaction arising from direct t_{2g}-t_{2g} overlap [16,17], which leads to a large Weiss temperature, $|\theta| \sim 1000$ K [6]. However, because of geometrical frustration inherent to the B-site network of the spinel lattice, this interaction does not produce a stable spin ordering in the cubic phase, and spin ordering ($T_N = 40$ K) occurs only after a structural phase transition occurs ($T_s = 50$ K) [10,15]. This structural phase transition into a tetragonal symmetry ($a > c$, similar to that of MnV_2O_4) can be regarded as an orbital ordering of V ions, and several different models have been proposed so far on this orbital ordering. Among them, two models are based on the Kugel-Khomskii-type coupling on the V site [11,18] but assume different types of orbital ordering. The third one [19] is based on spin-orbit coupling and cooperative Jahn-Teller coupling and predicts ferro-orbital ordering.

In MnV_2O_4, in addition to the strong antiferromagnetic V-V interaction, there is a superexchange antiferromagnetic interaction between Mn and V (A-B interaction) via oxygen in between, and this is responsible for the ferrimagnetic ordering ($T_N = 56.5$ K) in this compound. This ferrimagnetic state gives a ferromagnetic configuration of V spins, and thereby it affects the orbital state of the V site. Generally, a ferromagnetic spin configuration prefers a staggered-type orbital configuration (''antiferro-orbital'' ordering), and, therefore, a plausible scenario is that the evolution of ferromagnetic moment on the V site induces the enhancement of the antiferro-orbital interaction, resulting in the lattice contraction below $T_N = 56.5$ K and eventual orbital ordering below $T_s = 53.5$ K. The experimental result on the magnetic-field dependence can be explained by the same scenario; the applied magnetic field enhances the evolution of ferromagnetic moment on the V site and, thus, induces the orbital ordering and the structural phase transition into a tetragonal phase.

Substitution effect on MnV_2O_4 reveals a characteristic of orbital ordering in this V spinel. Figure 4 shows the T

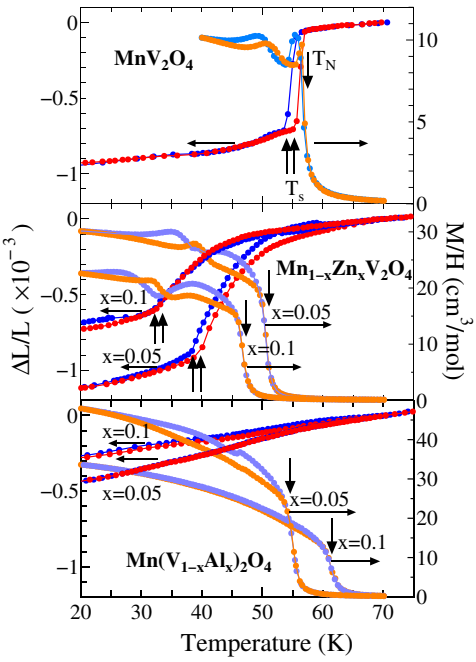

FIG. 4 (color online). Temperature dependence of lattice striction $\Delta L/L$ (left axis) and magnetization M under 100 G (right axis) for (a) MnV_2O_4, (b) $Mn_{1-x}Zn_xV_2O_4$, and (c) $Mn(V_{1-x}Al_x)_2O_4$. M is given per MnV_2O_4 mole.

dependence of M and $\Delta L/L$ in (a) MnV_2O_4, (b) with Zn^{2+} substitution for the Mn^{2+} site, and (c) with Al^{3+} substitution for the V^{3+} site. When the parent compound and $Mn_{1-x}Zn_xV_2O_4$ are compared, both T_N and T_s decrease with Zn substitution. The decrease of T_N can be explained by the decrease of the number of Mn spins. Associated with the suppression of T_N, T_s is also lowered but still exists in the Mn-site substituted samples. The size of magnetization increases with Zn doping, suggesting that the canting angle of the triangular structure changes with Zn doping. It is to be noted that the deviation between cooling and warming runs exists far above T_s for the striction measurement of Zn-doped samples, indicating that, though a global crystal structure is cubic, a local lattice distortion is occurring even above T_s. On the other hand, the behavior of the V-site substituted samples is totally different. As shown in Fig. 4(c), T_N does not substantially decrease, or it even increases with Al substitution for the V site. Furthermore, both the decrease of $\Delta L/L$ and the dip of M are smeared out, but they exhibit a monotonic T dependence below T_N in $Mn(V_{1-x}Al_x)_2O_4$, indicating that T_s disappears with the V-site substitution.

Similar fragility of the structural phase transition against disorder was observed in the charge/orbital ordering of perovskite manganites [20]. In those compounds, a small amount of Cr^{3+} impurities (with no orbital degrees of freedom) on the Mn^{3+} site ($3d^4$) act as a random field on the Mn orbital and suppress the long-range charge/orbital ordering. We can interpret the result of $Mn(V_{1-x}Al_x)_2O_4$ in the same way; the Al ions with no orbital degrees of freedom act as a random field on the V orbital and suppress the V orbital ordering. Such a substantial effect of a small amount of impurities indicates that the structural phase transition from a cubic to a tetragonal phase is a cooperative phenomenon dominated by orbital degrees of freedom.

Finally, we discuss the anisotropy of lattice striction against the direction of the magnetic field. As shown in Fig. 3(d), negative magnetostriction occuring around the transition temperatures ($T_N = 56.5$ K and $T_s = 53.5$ K) is almost the same for both $\Delta L/L \perp H$ and $\Delta L/L \parallel H$. However, there is another magnetostriction below T_N and T_s, as shown in Fig. 3(d), which is enhanced with decreasing T. This magnetostriction at low T is heavily anisotropic against the direction of H. Namely, the lattice is contracted along the direction of the magnetic field but is elongated perpendicular to it. Though its magnitude ($\Delta L/L \sim 10^{-3}$) is extremely large, this can be regarded as conventional magnetostriction, which is primarily dominated by single-ion spin-orbit coupling. These results indicate that different mechanisms work for the magnetoelastic phenomena at different temperature ranges in orbital-spin coupled systems such as MnV_2O_4.

We thank Y. Motome for fruitful discussions. This work was partly supported by a Grant-in-Aid for The 21st Century COE Program at Waseda University and by Grant-in-Aid for scientific research on priority area, both from MEXT of Japan.

[1] K. I. Kugel and D. I. Khomskii, Zh. Eksp. Teor. Fiz. **64**, 369 (1973) [Sov. Phys. JETP **37**, 725 (1973)].
[2] A. J. Millis, Nature (London) **392**, 147 (1998).
[3] T. Kimura *et al.*, Nature (London) **426**, 55 (2003).
[4] N. Hur *et al.*, Nature (London) **429**, 392 (2004).
[5] Y. Ren *et al.*, Nature (London) **396**, 441 (1998).
[6] Y. Ueda, N. Fujiwara, and H. Yasuoka, J. Phys. Soc. Jpn. **66**, 778 (1997).
[7] R. Plumier and M. Sougi, Solid State Commun. **64**, 53 (1987).
[8] R. Plumier and M. Sougi, Physica (Amsterdam) **155B**, 315 (1989).
[9] E. Nishibori *et al.*, Nucl. Instrum. Methods Phys. Res., Sect. A **467–468**, 1045 (2001).
[10] S.-H. Lee *et al.*, Phys. Rev. Lett. **93**, 156407 (2004).
[11] H. Tsunetsugu and Y. Motome, Phys. Rev. B **68**, 060405 (2003).
[12] In x-ray powder diffraction measurement, the superlattice peak whose intensity is less than 10^{-4} times that of the fundamental peaks cannot be detected.
[13] A. Asamitsu *et al.*, Nature (London) **373**, 407 (1995).
[14] H. Kuwahara *et al.*, Science **270**, 961 (1995).
[15] M. Reehuis *et al.*, Eur. Phys. J. B **35**, 311 (2003).
[16] J. B. Goodenough, Phys. Rev. **117**, 1442 (1960).
[17] H. F. Pen *et al.*, Phys. Rev. Lett. **78**, 1323 (1997).
[18] D. I. Khomskii and T. Mizokawa, Phys. Rev. Lett. **94**, 156402 (2005).
[19] O. Tchernyshyov, Phys. Rev. Lett. **93**, 157206 (2004).
[20] T. Katsufuji *et al.*, J. Phys. Soc. Jpn. **68**, 1090 (1999).